

## Vibration Suppression of an Elastic Plate by Use of an Electrorheological Patch and Constraining Layer

M. E. Aryaee panah\* and Seyyed M. Hasheminejad

*\*Acoustics Research Laboratory, Department of Mechanical Engineering  
Iran University of Science and Technology, Narmak, Tehran 16844 Iran*

### Abstract

Electrorheological materials are a class of smart materials which exhibit dramatic changes in mechanical properties (like shear modulus) due to strong applied external electric fields. In this paper forced harmonic vibration of a simply supported rectangular elastic plate with a rectangular ER patch with arbitrary size and location on the plate and a constraining layer on the patch is investigated. A dynamic model for the electric field-dependent frequency response of a rectangular plate and the ER patch and its constraining layer is developed. Hamilton's principle and the classical thin plate theory are applied to derive a set of fully coupled dynamic equations of motion along with the associated general boundary conditions. The frequency response functions and the modal loss factors are subsequently determined. The effects of electric field intensity, patch size and patch location on the frequency response functions and modal loss factors are investigated in numerical results. This work represents a rigorous analytical solution for the problem of the ER patch which seems to be absent in the previous works.

**Keywords:** Smart structures; Electrorheological; Semi active control; ER patch; vibration suppression

### 1. Introduction

Passive and active control are two ways of vibration suppression in engineering structures. In passive control the material properties of the structure itself, such as damping and stiffness, are modified so as to change the structural response (Saravanos and Chamis 1992). However, the material properties of such structures are predetermined in their design or construction phase, which can be hardly adapted to unexpected environmental changes. In order to overcome this disadvantage, intelligent materials such as piezoelectric materials or electro-rheological materials (ERs) may be incorporated into conventional structures in order to adapt to the changes of the environment. The latter materials have recently gained increasing popularity, as their rheological properties can rapidly and reversibly be varied when subjected to an electrical field (Winslow 1949). In particular, adaptive structures utilizing tunable ERFs have the beneficial control capabilities of simultaneously changing the damping and stiffness of the system by application of an electric field, in addition to the other valuable features of low-energy loss and easy controllability by computers (Weiss 1993).

Numerous investigators have thoroughly studied the use of smart ERF-based structures for vibration control in various spheres of engineering. The most significant contributions relevant to the present study shall be briefly reviewed here. Early investigations of the ER material in the structural vibration control problems can be traced to Coulter and coworkers (1989), (See also Coulter 1993), who performed theoretical and experimental studies of flexural vibrations of ER fluid-based sandwich beams. They found a good qualitative agreement between their model and experimental results, and observed that both natural frequencies and loss factors increase with increases in electric field. Choi et al. (1992) experimentally studied the vibration characteristics of ERF-based cantilevered beams. Also many other researchers such as Yeh et al. (2004) have studied the natural frequencies of adaptive ER-based plates and beams by means of numerical methods such as Rayleigh-Ritz. A few researchers like Kung and Singh (1998) have investigated the effect of partially covered sandwich plates with viscoelastic cores in the same way.

The above review indicates that while there exists a notable body of literature on free vibration characteristics of electrorheological fluid-based sandwich plates, rigorous analytical solutions for the vibrational response of such structures seems to be absent, especially in case of partially covered plates. The primary purpose of the current work is to fill this gap. Thus, in this paper, we use Hamilton's principle and the classical thin plate theory to present a closed

\*Email: peyman.aryaee@gmail.com

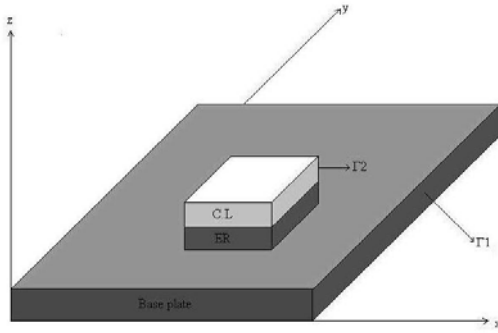
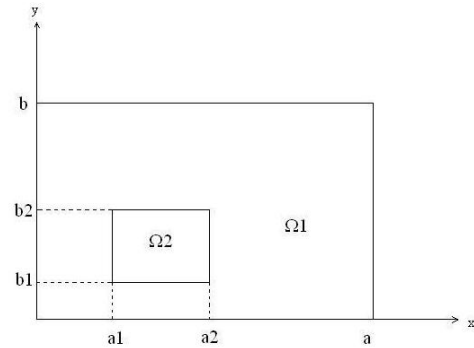


Figure 1. Problem geometry

Figure 2.  $\Omega_1$  and  $\Omega_2$  regions

form Fourier series solution for harmonic transverse vibration of a simply-supported rectangular plate with an ER patch. The proposed model is of noble interest basically due to its inherent value as a canonical problem in structural dynamics. It is also of practical value for vibration control engineers involved in development of reliable analytical and/or experimental tools for the design and analysis of ER-based plates or panels with optimal vibrational characteristics. As it was said, this solution has the capability of using a patch with arbitrary size and position on the base plate.

## 2. Formulation

### 2.1 Basic relations

The complete configuration of the sandwich rectangular plate consisting of a base plate (thickness  $h_3$ ), a constraining layer (thickness  $h_1$ ), and a tunable ER material core layer (thickness  $h_2$ ) is illustrated in Figure 1 and Figure 2. The base and constraining layers are initially assumed to be undamped, cross-ply elastic composite laminates, with width  $a$  and length  $b$ .

It is assumed that there is no slipping between the elastic and ER layers. The transverse displacements, of every point on a cross-section of the plate, including the points under the patch, are assumed to be the same. Furthermore, there exists no normal stress in the ER layer as well as no transverse shear strains in the laminated layers 1 and 3. The above kinematical assumptions imply that the total displacement components at a material point  $(x, y, z)$  within the upper and lower elastic laminates may be expressed as (see Figure 3):

$$\begin{aligned} u^{(i)}(x, y, z) &= u_i(x, y) - z_i \frac{\partial w}{\partial x} \\ v^{(i)}(x, y, z) &= v_i(x, y) - z_i \frac{\partial w}{\partial y} \\ w^{(i)}(x, y, z) &= w(x, y) \end{aligned} \quad (1)$$

Where  $z_i$  ( $i = 1, 3$ ) is the transverse coordinate in the local coordinate system of the upper and lower layers positioned at their associated mid-planes, and  $u_i(x, y)$  and  $v_i(x, y)$  are the mid-plane deformations in the  $x$  and  $y$  directions, respectively. Assuming linear strain-displacement relations, the strain components in the elastic cross-ply laminated layers can be expressed as

$$\begin{aligned} \varepsilon_x^{(i)} &= \frac{\partial u_i}{\partial x} - z_i \frac{\partial^2 w}{\partial x^2}, \quad \varepsilon_y^{(i)} = \frac{\partial v_i}{\partial y} - z_i \frac{\partial^2 w}{\partial y^2} \\ \gamma_{xy}^{(i)} &= \frac{\partial u_i}{\partial y} + \frac{\partial v_i}{\partial x} - 2z_i \frac{\partial^2 w}{\partial x \partial y} \end{aligned} \quad (2)$$

Where  $i = 1, 3$ . Also, the transverse shear strain components in the ER fluid (layer 2), as illustrated in Figures. 3a and 3b, are written as (Yeh and Chen 2004)

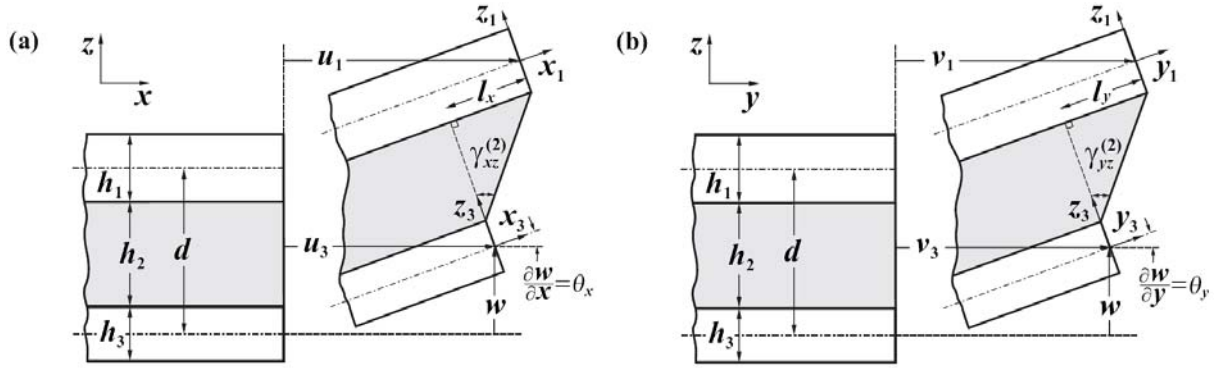


Figure 3. Geometrical constraints between 3 layers

$$\gamma_{xz}^{(2)} = \frac{l_x}{h_2} = \frac{d}{h_2} \frac{\partial w}{\partial x} + \frac{(u_1 - u_3)}{h_2} \quad (3)$$

$$\gamma_{yz}^{(2)} = \frac{l_y}{h_2} = \frac{d}{h_2} \frac{\partial w}{\partial y} + \frac{(v_1 - v_3)}{h_2}$$

Where  $l_x = d\theta_x + (u_1 - u_3)$ ,  $l_y = d\theta_y + (v_1 - v_3)$ , in which  $d = h_1/2 + h_2 + h_3/2$ .

In addition, assuming a state of plane stress within the upper and lower cross-ply laminates (i.e., layers 1 and 3) entails that the stress components within the  $k$ -th orthotropic lamina in each elastic layer can be obtained from Hooke's law as (Reddy 2003):

$$\begin{Bmatrix} \sigma_x^{(i)} \\ \sigma_y^{(i)} \\ \sigma_{xy}^{(i)} \end{Bmatrix}^{(k)} = \begin{bmatrix} \bar{Q}_{11}^{(i)} & \bar{Q}_{12}^{(i)} & 0 \\ \bar{Q}_{12}^{(i)} & \bar{Q}_{22}^{(i)} & 0 \\ 0 & 0 & \bar{Q}_{66}^{(i)} \end{bmatrix}^{(k)} \begin{Bmatrix} \varepsilon_x^{(i)} \\ \varepsilon_y^{(i)} \\ \gamma_{xy}^{(i)} \end{Bmatrix} \quad (4)$$

Where  $\bar{Q}_{\alpha\beta}^{(i)}$  ( $i=1,3$ ) represent the reduced transformed elastic constants in each orthotropic lamina within the  $i$ -th layer which in the case of isotropic materials reduce to

$$\bar{Q}_{11}^{(i)} = \bar{Q}_{22}^{(i)} = \frac{E_i}{1-\nu_i^2}, \quad \bar{Q}_{12}^{(i)} = \frac{\nu_i E_i}{1-\nu_i^2}, \quad \bar{Q}_{66}^{(i)} = \frac{E_i}{2(1+\nu_i)} \quad (5)$$

Where  $E_i$  and  $\nu_i$  are the corresponding Young modulus and Poisson ratio, respectively. Like most of the papers on the usage of ER materials in adaptive structures, this paper considers ER material as a viscoelastic material, and complex modulus is used to identify the shear properties of the material in harmonic oscillation. So the transverse shear stresses in the ER fluid are written as (Yeh and Chen 2004):

$$\sigma_{xz}^{(2)} = G^{(2)} \gamma_{xz}^{(2)},$$

$$\sigma_{yz}^{(2)} = G^{(2)} \gamma_{yz}^{(2)}, \quad (6)$$

Where  $G^{(2)}$  is the viscoelastic shear modulus of the ER fluid layer.

## 2.2 Equations of motion and boundary conditions

In this subsection, Hamilton's principle is employed to derive the governing equations of motion for the total system along with the associated edge boundary conditions in general form. Following the standard procedure, we shall extremize (make stationary) the time integral of the Lagrangian for the entire system in any arbitrarily time interval, i.e.,

$$\delta I = \delta \int_{t_1}^{t_2} L dt = \delta \int_{t_1}^{t_2} (T - U + W) dt = 0 \quad (7)$$

Where  $\delta$  denotes the first variation operator,  $W$  represents the work done by the external forces, and  $L$ ,  $U$ , and  $T$  are the Lagrangian, total strain energy, and total kinetic energy of the sandwich plate, respectively. Also, keeping in

mind the state of plane stress throughout the upper and lower laminates in addition to the absence of normal stresses in the ER core layer, the variation of the total strain energy can be written as

$$\begin{aligned} \delta U &= \sum_{i=1,3} \int_{\Omega_i} (\sigma_x^{(i)} \delta \epsilon_x^{(i)} + \sigma_y^{(i)} \delta \epsilon_y^{(i)} + \sigma_{xy}^{(i)} \delta \gamma_{xy}^{(i)}) dV_i + \int_{V_2} (\sigma_{xz}^{(2)} \delta \gamma_{xz}^{(2)} + \sigma_{yz}^{(2)} \delta \gamma_{yz}^{(2)}) dV_2 \\ &= \sum_{i=1,3} \int_{\Omega_i} (N_x^{(i)} \delta \epsilon_x^{(i)} + N_y^{(i)} \delta \epsilon_y^{(i)} + N_{xy}^{(i)} \delta \gamma_{xy}^{(i)}) d\Omega_i + \int_{\Omega_2} (Q_x^{(2)} \delta \gamma_{xz}^{(2)} + Q_y^{(2)} \delta \gamma_{yz}^{(2)}) d\Omega_2 \end{aligned} \quad (8)$$

where  $V_1$ ,  $V_2$  and  $V_3$  denote the three dimensional domains for the upper elastic layer 1, ER core layer 2, and lower elastic layer 3, respectively,  $\Omega_1$  signifies the two dimensional ( $a \times b$ ) surface of the base plate and  $\Omega_2 = \Omega_3$  stands for the patch area in the  $x$ - $y$  plane (see Figure 2). Also, the relevant stress resultants within the upper, lower and core layers, appearing in the above relations are defined as:

$$(N_x^{(i)}, N_y^{(i)}, N_{xy}^{(i)}) = \int_{-h_i/2}^{h_i/2} (\sigma_x^{(i)}, \sigma_y^{(i)}, \sigma_{xy}^{(i)}) dz_i \quad (i = 1, 3) \quad (9a)$$

$$(Q_x^{(2)}, Q_y^{(2)}) = \int_{-h_2/2}^{h_2/2} (\sigma_{xz}^{(2)}, \sigma_{yz}^{(2)}) dz_2 \quad (9b)$$

Where  $z_2$  is the transverse coordinate in the local coordinate system of the ER core layer positioned at its mid-plane. Next, having adopted the classical thin plate theory and neglecting the rotational inertia (in-plane components of the kinetics energy) of the elastic layers, the variation of the total kinetic energy of the sandwich plate can be written as:

$$\delta T = \sum_{i=1,3} \delta \int_{\Omega_i} \frac{1}{2} \rho_i h_i (\dot{u}_i^2 + \dot{v}_i^2 + \dot{w}_i^2) d\Omega_i + \delta \int_{\Omega_2} \frac{1}{2} \left\{ \rho_2 h_2 \dot{w}_2^2 + I_2 [(\dot{\gamma}_{xz}^{(2)})^2 + (\dot{\gamma}_{yz}^{(2)})^2] \right\} d\Omega_2 \quad (10)$$

Where  $\rho_i$  ( $i = 1, 2, 3$ ) denotes the mass density in the  $i$ -th layer, and  $I_2 (= \rho_2 h_2^3 / 12)$  is the mass moment of inertia of the ER fluid interlayer. Also, when the sandwich plate is subjected to an external transverse distributed force,  $q(x, y, t)$  the variation of the total work done by the external force  $\dot{W}$  is given as

$$\delta \dot{W} = \int_{\Omega_2} q' \delta w d\Omega_2 + \int_{\Omega_1 - \Omega_2} q'' \delta w d(\Omega_1 - \Omega_2) \quad (11)$$

In which,  $q'$  is the portion of the force which acts on the patch area and  $q''$  is the portion of the force which acts on the rest of the elastic plate.

Next, substitution of the strain-displacement relations (2) and (3) in (8) yields

$$\begin{aligned} \delta U &= \sum_{i=1,3} \int_{\Omega_i} \left[ N_x^{(i)} \left( \frac{\partial \delta u_i}{\partial x} \right) - M_x^{(i)} \left( \frac{\partial^2 \delta w}{\partial x^2} \right) + N_y^{(i)} \left( \frac{\partial \delta v_i}{\partial y} \right) \right. \\ &\quad \left. - M_y^{(i)} \left( \frac{\partial^2 \delta w}{\partial y^2} \right) + N_{xy}^{(i)} \left( \frac{\partial \delta u_i}{\partial y} + \frac{\partial \delta v_i}{\partial x} \right) - 2M_{xy}^{(i)} \left( \frac{\partial^2 \delta w}{\partial x \partial y} \right) \right] d\Omega_i \\ &\quad + \int_{\Omega_2} \left[ Q_x^{(2)} \left( \frac{d}{h_2} \frac{\partial \delta w}{\partial x} + \frac{\delta u_1 - \delta u_3}{h_2} \right) + Q_y^{(2)} \left( \frac{d}{h_2} \frac{\partial \delta w}{\partial y} + \frac{\delta v_1 - \delta v_3}{h_2} \right) \right] d\Omega_2 \end{aligned} \quad (12)$$

Where the pertinent moment resultants in the above relation are defined as:

$$(M_x^{(i)}, M_y^{(i)}, M_{xy}^{(i)}) = \int_{-h_i/2}^{h_i/2} (\sigma_x^{(i)}, \sigma_y^{(i)}, \sigma_{xy}^{(i)}) z_i dz_i \quad (i = 1, 3) \quad (13)$$

Similarly, substitution of the strain-displacement relations (3) in (10) and performing time integration by parts, yields

$$\begin{aligned} \delta \int_{t_1}^{t_2} T dt &= - \sum_{i=1,3} \int_{t_1}^{t_2} \int_{\Omega_i} \rho_i h_i (\ddot{u}_i \delta u_i + \ddot{v}_i \delta v_i + \ddot{w}_i \delta w) d\Omega_i dt \\ &\quad - \int_{t_1}^{t_2} \int_{\Omega_2} \left[ \rho_2 h_2 \dot{w}_2 \delta w + I_2 \left( \frac{d}{h_2} \frac{\partial \dot{w}}{\partial x} + \frac{\dot{u}_1 - \dot{u}_3}{h_2} \right) \left( \frac{d}{h_2} \frac{\partial \delta w}{\partial x} + \frac{\delta u_1 - \delta u_3}{h_2} \right) \right. \\ &\quad \left. + I_2 \left( \frac{d}{h_2} \frac{\partial \dot{w}}{\partial y} + \frac{\dot{v}_1 - \dot{v}_3}{h_2} \right) \left( \frac{d}{h_2} \frac{\partial \delta w}{\partial y} + \frac{\delta v_1 - \delta v_3}{h_2} \right) \right] d\Omega_2 dt \end{aligned} \quad (14)$$

Now, employing (11), (12), and (14) into Hamilton's principle (Eq. 7), and making use of the so-named gradient theorem, while taking advantage of the fundamental lemma of calculus of variations (Forsyth 1960) results into the general form of equations of motion for forced vibration of the ERF-based sandwich plate:

in  $\Omega_1$  :

$$\begin{aligned}
\delta u_1 : & -\rho_1 h_1 \ddot{u}_1 + \frac{\partial N_x^{(1)}}{\partial x} + \frac{\partial N_{xy}^{(1)}}{\partial y} = 0 \\
\delta v_1 : & -\rho_1 h_1 \ddot{v}_1 + \frac{\partial N_y^{(1)}}{\partial y} + \frac{\partial N_{xy}^{(1)}}{\partial x} = 0 \\
\delta w : & -\rho_1 h_1 \ddot{w} + \frac{\partial^2 M_x^{(1)}}{\partial x^2} + \frac{\partial^2 M_y^{(1)}}{\partial y^2} + 2 \frac{\partial^2 M_{xy}^{(1)}}{\partial x \partial y} + q''(x, y, t) = 0
\end{aligned} \tag{15a}$$

In  $\Omega_2$  :

$$\begin{aligned}
\delta u_1 : & \frac{-I_2 d}{(h_2)^2} \frac{\partial \ddot{w}}{\partial x} - \frac{I_2}{(h_2)^2} \ddot{u}_1 + \frac{I_2}{(h_2)^2} \ddot{u}_3 - \frac{1}{h_2} Q_x^{(2)} = 0 \\
\delta u_3 : & -\rho_3 h_3 \ddot{u}_3 + \frac{I_2 d}{(h_2)^2} \frac{\partial \ddot{w}}{\partial x} + \frac{I_2}{(h_2)^2} \ddot{u}_1 - \frac{I_2}{(h_2)^2} \ddot{u}_3 + \frac{\partial N_x^{(3)}}{\partial x} + \frac{\partial N_{xy}^{(3)}}{\partial y} + \frac{1}{h_2} Q_x^{(2)} = 0 \\
\delta v_1 : & -\frac{I_2 d}{(h_2)^2} \frac{\partial \ddot{w}}{\partial y} - \frac{I_2}{(h_2)^2} \ddot{v}_1 + \frac{I_2}{(h_2)^2} \ddot{v}_3 - \frac{1}{h_2} Q_y^{(2)} = 0
\end{aligned} \tag{15b}$$

$$\begin{aligned}
\delta v_3 : & -\rho_3 h_3 \ddot{v}_3 + \frac{I_2 d}{(h_2)^2} \frac{\partial \ddot{w}}{\partial y} + \frac{I_2}{(h_2)^2} \ddot{v}_1 - \frac{I_2}{(h_2)^2} \ddot{v}_3 + \frac{\partial N_y^{(3)}}{\partial y} + \frac{\partial N_{xy}^{(3)}}{\partial x} + \frac{1}{h_2} Q_y^{(2)} = 0 \\
\delta w : & -\rho_3 h_3 \ddot{w} - \rho_2 h_2 \ddot{w} + I_2 \left( \frac{d}{h_2} \right)^2 \frac{\partial^3 \ddot{w}}{\partial x^2} + \frac{I_2 d}{(h_2)^2} \frac{\partial \ddot{u}_1}{\partial x} - \frac{I_2 d}{(h_2)^2} \frac{\partial \ddot{u}_3}{\partial x} + I_2 \left( \frac{d}{h_2} \right)^2 \frac{\partial^3 \ddot{w}}{\partial y^2} \\
& + \frac{I_2 d}{(h_2)^2} \frac{\partial \ddot{v}_1}{\partial y} - \frac{I_2 d}{(h_2)^2} \frac{\partial \ddot{v}_3}{\partial y} + \frac{\partial^2 M_x^{(3)}}{\partial x^2} + \frac{\partial^2 M_y^{(3)}}{\partial y^2} + 2 \frac{\partial^2 M_{xy}^{(3)}}{\partial x \partial y} + \frac{d}{h_2} \frac{\partial Q_x^{(2)}}{\partial x} + \frac{d}{h_2} \frac{\partial Q_y^{(2)}}{\partial y} + q'(x, y, t) = 0
\end{aligned}$$

Along with the boundary conditions:

On  $\Gamma_1$  :

**Essential**

$$\delta u_1 = 0$$

or

**natural**

$$N_x^{(1)} n_x + N_{xy}^{(1)} n_y = 0$$

$$\tag{16a}$$

$$\delta v_1 = 0$$

or

$$N_y^{(1)} n_y + N_{xy}^{(1)} n_x = 0$$

$$\tag{16b}$$

$$\delta w = 0$$

or

$$\left( \frac{\partial M_x^{(1)}}{\partial x} + 2 \frac{\partial M_{xy}^{(1)}}{\partial y} \right) n_x + \left( \frac{\partial M_y^{(1)}}{\partial y} - 2 M_{xy}^{(1)} \right) n_y = 0$$

$$\tag{16c}$$

$$\delta \left( \frac{\partial w}{\partial x} \right) = 0$$

or

$$M_x^{(1)} n_x = 0$$

$$\tag{16d}$$

$$\delta \left( \frac{\partial w}{\partial y} \right) = 0$$

or

$$M_y^{(1)} n_y = 0$$

$$\tag{16e}$$

On  $\Gamma_2$  :

**Essential**

$$\delta u_3 = 0$$

or

$$N_x^{(3)} n_x + N_{xy}^{(3)} n_y = 0$$

$$\tag{16f}$$

$$\delta v_3 = 0$$

or

$$N_y^{(3)} n_y - N_{xy}^{(3)} n_x = 0$$

$$\tag{16g}$$

$$\delta w = 0$$

or

$$\begin{aligned}
& \left( -I_2 \left( \frac{d}{h_2} \right)^2 \frac{\partial \ddot{w}}{\partial x} - \frac{I_2 d}{(h_2)^2} \ddot{u}_1 + \frac{I_2 d}{(h_2)^2} \ddot{u}_3 \right. \\
& \left. - \frac{\partial M_x^{(3)}}{\partial x} - 2 \frac{\partial M_{xy}^{(3)}}{\partial y} - \frac{d}{h_2} Q_x^{(2)} \right) n_x \\
& + \left( -I_2 \left( \frac{d}{h_2} \right)^2 \frac{\partial \ddot{w}}{\partial y} - \frac{I_2 d}{(h_2)^2} \ddot{v}_1 + \frac{I_2 d}{(h_2)^2} \ddot{v}_3 \right. \\
& \left. - \frac{\partial M_y^{(3)}}{\partial y} + 2 M_{xy}^{(3)} - \frac{d}{h_2} Q_y^{(2)} \right) n_y = 0
\end{aligned} \tag{16h}$$

where  $n_x$  and  $n_y$  are the projections of the outward unit vector  $\mathbf{n}$  on the edge boundary of the plate in the  $x$  and  $y$  directions, respectively. One should note that for any of the above boundary conditions either the essential or the corresponding natural conditions should be satisfied.

Next, substitution of the strain-displacement (2) and (3) into the constitutive relations (4) and (6) and subsequent results into (9) and (13) leads to the expressions for the stress and moment resultants in terms of the displacement components as

$$\left. \begin{aligned} N_x^{(i)} &= A_{11}^{(i)} \frac{\partial u_i}{\partial x} + A_{12}^{(i)} \frac{\partial v_i}{\partial y} - B_{11}^{(i)} \frac{\partial^2 w}{\partial x^2} - B_{12}^{(i)} \frac{\partial^2 w}{\partial y^2}, & M_x^{(i)} &= B_{11}^{(i)} \frac{\partial u_i}{\partial x} + B_{12}^{(i)} \frac{\partial v_i}{\partial y} - D_{11}^{(i)} \frac{\partial^2 w}{\partial x^2} - D_{12}^{(i)} \frac{\partial^2 w}{\partial y^2} \\ N_y^{(i)} &= A_{12}^{(i)} \frac{\partial u_i}{\partial x} + A_{22}^{(i)} \frac{\partial v_i}{\partial y} - B_{12}^{(i)} \frac{\partial^2 w}{\partial x^2} - B_{22}^{(i)} \frac{\partial^2 w}{\partial y^2}, & M_y^{(i)} &= B_{12}^{(i)} \frac{\partial u_i}{\partial x} + B_{22}^{(i)} \frac{\partial v_i}{\partial y} - D_{12}^{(i)} \frac{\partial^2 w}{\partial x^2} - D_{22}^{(i)} \frac{\partial^2 w}{\partial y^2} \\ N_{xy}^{(i)} &= A_{66}^{(i)} \left( \frac{\partial u_i}{\partial y} + \frac{\partial v_i}{\partial x} \right) - 2B_{66}^{(i)} \frac{\partial^2 w}{\partial x \partial y}, & M_{xy}^{(i)} &= B_{66}^{(i)} \left( \frac{\partial u_i}{\partial y} + \frac{\partial v_i}{\partial x} \right) - 2D_{66}^{(i)} \frac{\partial^2 w}{\partial x \partial y} \\ Q_x^{(2)} &= G^{(2)} \left( d \frac{\partial w}{\partial x} + u_1 - u_3 \right), & Q_y^{(2)} &= G^{(2)} \left( d \frac{\partial w}{\partial y} + v_1 - v_3 \right) \end{aligned} \right\} \quad (17)$$

where  $i = 1, 3$ ; and the rigidity constants appearing in the above relations are defined as

$$(A_{jk}^{(i)}, B_{jk}^{(i)}, D_{jk}^{(i)}) = \int_{-h_i/2}^{h_i/2} (1, z_i, z_i^2) \bar{Q}_{jk} dz_i \quad (18)$$

in which the indices  $j$  and  $k$  can be 1, 2, or 6. One should notice that because the integrals in (9) and (13) are performed on each of the base or constraining layers separately, and  $z_i$  is considered with respect to each plate's mid plane  $B_{jk}^{(i)}$  is zero when each of the base or constraining layer plates are symmetrical with respect to its pertaining mid plane (Yeh and Chen 2004). Ultimately, substitution of (17) into (15) leads to the final form of the displacement equations of motion. We can combine the equations on  $\Omega_1$  and  $\Omega_2$  domains by use of Heaviside function. For example, the first equation of motion (related to  $u_1$ ) reads:

$$\begin{aligned} & A_{11}^{(1)} \frac{\partial^2 u_1}{\partial x^2} + A_{12}^{(1)} \frac{\partial^2 v_1}{\partial x \partial y} + A_{66}^{(1)} \left( \frac{\partial^2 u_1}{\partial y^2} + \frac{\partial^2 v_1}{\partial x \partial y} \right) - \rho_1 h_1 \ddot{u}_1 + \tilde{H}(x, y) \left( \frac{-I_2 d}{(h_2)^2} \frac{\partial \ddot{w}}{\partial x} \right. \\ & \left. - \frac{I_2}{(h_2)^2} \ddot{u}_1 + \frac{I_2}{(h_2)^2} \ddot{u}_3 - \frac{1}{h_2} G^{(2)} \left( d \frac{\partial w}{\partial x} + u_1 - u_3 \right) \right) = 0 \end{aligned} \quad (19)$$

where

$$\tilde{H}(x, y) = H(x - a_1, y - b_1) H(a_2 - x, b_2 - y) \quad (20)$$

In which  $H(x, y)$  is the Heaviside function and  $a_1$  and  $b_1$  denote the location and size of the patch, as it is depicted in Figure 2.

### 2.3 Frequency response

At this point, the frequency response of the rectangular plate and the patch is investigated. For the sake of simplicity, the straight edges of the plate at  $x = (0, a)$  and  $y = (0, b)$  are all assumed to be simply-supported. Thus, keeping the general boundary conditions (16) in view, one must consider the essential boundary conditions

$$\begin{aligned} & u_i(x, 0, t) = u_i(x, b, t) = v_i(0, y, t) = v_i(a, y, t) = 0 \quad (i = 1, 3) \\ & w(x, 0, t) = w(x, b, t) = w(0, y, t) = w(a, y, t) = 0 \\ & \partial w(x, 0, t) / \partial x = \partial w(x, b, t) / \partial x = \partial w(0, y, t) / \partial y = \partial w(a, y, t) / \partial y = 0 \end{aligned} \quad (21a)$$

in addition to the natural boundary conditions:

$$\begin{aligned} & N_x^{(i)}(0, y, t) = N_x^{(i)}(a, y, t) = N_y^{(i)}(x, 0, t) = N_y^{(i)}(x, b, t) = 0 \quad (i = 1, 3) \\ & M_x^{(1)}(0, y, t) + M_x^{(3)}(0, y, t) = M_x^{(1)}(a, y, t) + M_x^{(3)}(a, y, t) = 0 \\ & M_y^{(1)}(x, 0, t) + M_y^{(3)}(x, 0, t) = M_y^{(1)}(x, b, t) + M_y^{(3)}(x, b, t) = 0 \end{aligned} \quad (21b)$$

As it was mentioned in section 2.1, the transverse displacement across the whole width of the sandwich plate is assumed to be the same, and it is independent of the thickness coordinate. This assumption is based on the use of classical thin plate theory for the base and constraining plate layers and the incompressibility of the core. So displacement components  $u_i$ ,  $v_i$ , and  $w$ , which identically satisfy all above essential and natural boundary conditions, may advantageously be expanded as double Fourier series in the form

$$\begin{aligned} u_i(x, y, t) &= \sum_{n=1}^{\infty} \sum_{m=1}^{\infty} u_{mn}^{(i)}(t) \cos(\alpha_m x) \sin(\beta_n y) \\ v_i(x, y, t) &= \sum_{n=1}^{\infty} \sum_{m=1}^{\infty} v_{mn}^{(i)}(t) \sin(\alpha_m x) \cos(\beta_n y) \\ w(x, y, t) &= \sum_{n=1}^{\infty} \sum_{m=1}^{\infty} w_{mn}(t) \sin(\alpha_m x) \sin(\beta_n y) \end{aligned} \quad (22)$$

where  $u_{mn}^{(i)}(t)$ ,  $v_{mn}^{(i)}(t)$  ( $i=1,3$ ), and  $w_{mn}(t)$  are unknown functions of time to be determined, and  $\alpha_m = m\pi/a$ ,  $\beta_n = n\pi/b$ .

Substitution of equations (22) in the equations of motion and using the orthogonality of trigonometric functions yield five coupled ordinary differential equations in the time domain. Taking the Fourier transform of these five differential equations leads to the following matrix form:

$$\mathbf{Z}_{mn} \boldsymbol{\xi}_{mn} = \mathbf{q}_{mn} \quad (23)$$

Where

$$\begin{aligned} \boldsymbol{\xi}_{mn} &= [U_{mn}^{(1)}(\omega), U_{mn}^{(3)}(\omega), V_{mn}^{(1)}(\omega), V_{mn}^{(3)}(\omega), W_{mn}(\omega)]^T \\ \mathbf{q}_{mn} &= [0, 0, 0, 0, q_{mn}(\omega)]^T \end{aligned} \quad (24)$$

In which  $q_{mn}(\omega)$  is the Fourier transform of the forcing function, and  $U_{mn}^{(i)}(\omega)$ ,  $V_{mn}^{(i)}(\omega)$  and  $W_{mn}(\omega)$  are the Fourier transforms of the unknown displacement functions  $u_{mn}^{(i)}(t)$ ,  $v_{mn}^{(i)}(t)$  and  $w_{mn}(t)$ . Clearly, the unknown frequency functions in  $\boldsymbol{\xi}_{mn}$  can readily be determined from (23) in the form  $\boldsymbol{\xi}_{mn} = \mathbf{Z}_{mn}^{-1} \mathbf{q}_{mn}$ . Indeed the external force may have any kind of time dependence (and consequently  $q_{mn}(\omega)$  may have any kind of frequency dependence) but when one considers a unit impulse ( $\delta(t)$ ) as the applied force at a point on the plate which is not located at a nodal line, the frequency response functions will show all of the natural frequencies with correct amplitude.

To validate our solution we assumed the dimensions of the patch so as to reach to a fully covered sandwich plate, and we compared the natural frequencies with those of Hasheminejad and Maleki (2009). As it can be seen in table 1 very good coincidence were found between the results in this case.

Table 1. Comparison of natural frequencies of the fully covered sandwich plate with previous researches

Mode number	Reference	b/a=1 , E=0	b/a=4, E=3.5
(1,1)	Present study	13.1939	467.239
	Hasheminejad & Maleki	13.1925	467.2367
(2,1)	Present study	32.9849	145.651
	Hasheminejad & Maleki	32.98	145.6540

### 3. Numerical results

In order to investigate the effect of an ER path, and its size and location, on the natural frequencies and loss factors of an elastic plate we consider 12 cases (table 2). In all cases the base plate properties are:  $a = 1m$ ,  $b = 0.5m$ ,  $h_3 = 1mm$ ,  $\rho_3 = 2700Kg/m^3$ ,  $E_3 = 70GPa$ . Also the ER and constraining layer's thicknesses and material properties are constant in all cases,  $h_2 = 3mm$ ,  $h_1 = 0.5mm$ ,  $\rho_2 = 1700Kg/m^3$ ,  $\rho_3 = 2700Kg/m^3$  and  $E_3 = 70GPa$ . One should note that because the base and constraining layers are both isotropic and therefore symmetric with respect to their pertaining mid planes  $B_{jk}^{(i)}$  is zero. For example,  $B_{jk}^{(1)} = \int_{-h_1/2}^{h_1/2} z_1 \bar{Q}_{jk} dz_1$  and because the constraining layer is isotropic,  $\bar{Q}_{jk}$  is independent of  $z_1$  and hence  $B_{jk}^{(1)} = 0$ .

The complex modulus for a typical ER fluid is given, for example, by Yalcintas and Coulter (1995) which is expressed as follows:

$$G^{(2)} = G'(E) + iG''(E) \quad (25)$$

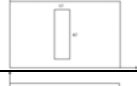
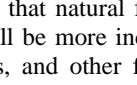
Where  $G'(E) = 50,000E^2$  is the shear storage modulus,  $G''(E) = 2600E + 1700$  is the loss modulus, and  $E$  is the electric field strength in kV/mm. The patch size and location and the electric field intensity for all cases are given in table 2.

In all cases impulse force is applied at the point  $(\frac{4}{10}a, \frac{25}{100}b)$  and the displacement of the point  $(\frac{7}{10}a, \frac{65}{100}b)$  is considered.

One should note that the force and displacement positions mainly affect on the amplitude of the FRF's.

Firstly we investigate the effect of a square patch in the center of a rectangular plate. Figures 4 and 5 show the frequency response functions and the modal loss factors of the plate without patch (case 1), a plate with a  $10 \times 10 \text{ cm}^2$  patch in the center (case 2) and a plate with a  $20 \times 20 \text{ cm}^2$  patch in the center (case 3). The electric field intensity is 1 Kv/mm in both cases. As it can be seen from figures, a decrease in natural frequencies is observed when a patch at the center of the plate with  $E=1 \text{ Kv/mm}$  is used, and there will be more decrease in natural frequencies when the size of the patch is increased. Also, it can be seen that for the first vibration mode, modal loss factor decreases as the size of the patch increases, but for the second mode, increasing the size of the patch results in an increase in modal loss factor. For the other four modes, the modal loss factor of the plate with the smaller patch is more than that of the plate with the larger patch.

Table 2. Different investigated cases

Case No.	$a_1$ (cm)	$a_2$ (cm)	$b_1$ (cm)	$b_2$ (cm)	E (Kv/mm)	
1	-	-	-	-	-	
2	45	55	20	30	1	
3	40	60	15	35	1	
4	45	55	20	30	3	
5	40	60	15	35	3	
6	45	55	5	45	3	
7	30	70	20	30	3	
8	90	100	40	50	3	
9	60	70	30	40	3	
10	80	100	30	50	3	
11	65	85	15	35	3	
12	46	54	0	50	3	

Now, we increase the electric field intensity by 3 Kv/mm. Figure 6 shows that natural frequencies will increase when we apply a  $10 \times 10 \text{ cm}^2$  patch in the center of the base plate, and there will be more increase when we apply a  $20 \times 20$  patch. But this pattern changes after the first three natural frequencies, and other frequencies will decrease by applying the patch in the center of the plate. As it can be seen from Figure 7, modal loss factors generally

decrease when the electric field is increased to 3 Kv/mm, and the loss factor of the plate with smaller patch is less than that of the plate with larger patch in all modes except the fifth mode.

To see the effect of the patch location, we consider cases 5, 10 and 11. From Figure 8 we see that the frequency response function of cases 5 and 11 are exactly the same, but there is a little decrease in natural frequencies of case 10 with respect to these two cases. But the effect of the patch location is a little different when we use a 10\*10 patch. Figure 10 shows the frequency response function of cases 4, 8 and 9. We can see that for a 10\*10 patch, the location of the patch has more effect on the first two natural frequencies, than that of a 20\*20 patch. As it can be seen in Figure 9, the modal loss factor of the cases 5 and 11 are the same for all mode numbers except the fifth mode. As it can be seen from Figure 11, the location of the patch becomes more effective when the patch size is decreased to 10\*10 cm.

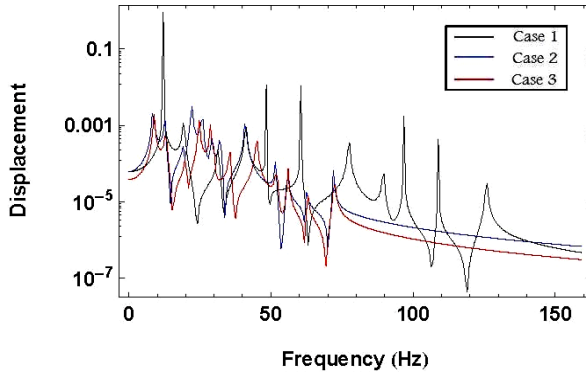


Figure 4. Frequency response of cases 1, 2 and 3

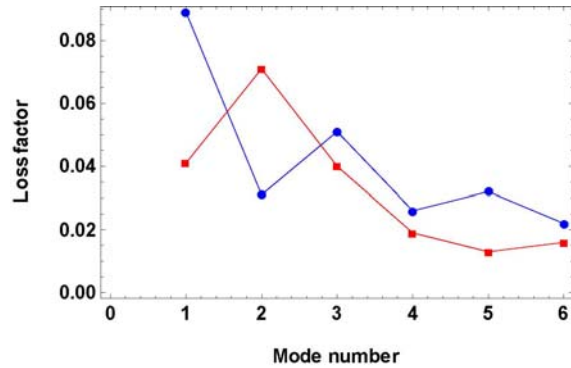


Figure 5. Modal loss factor of cases 2 and 3

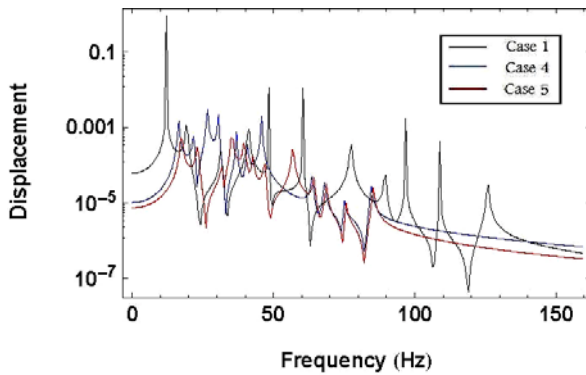


Figure 6. Frequency response of cases 1, 4 and 5

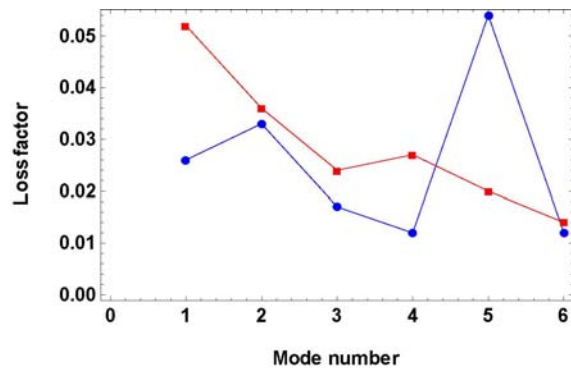


Figure 7. Modal loss factor of cases 4 and 5

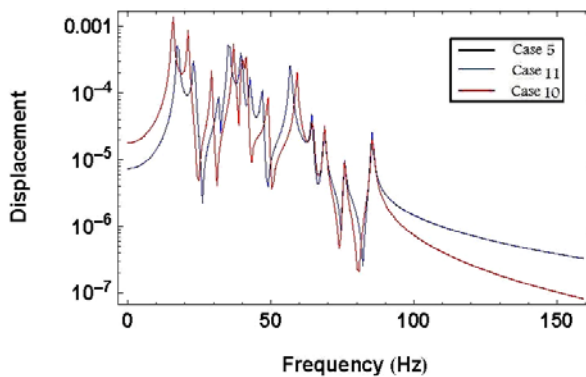


Figure 8. Frequency response of cases 5, 11 and 10

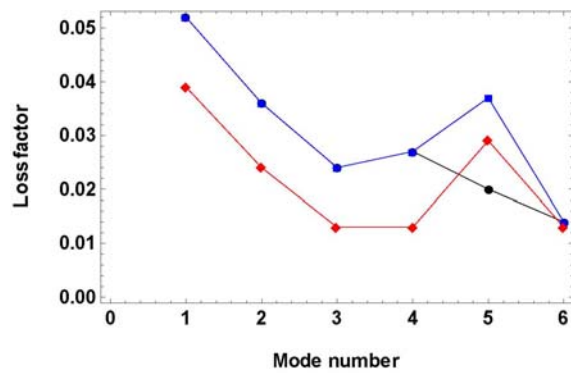


Figure 9. Modal loss factor of cases 5, 11 and 10

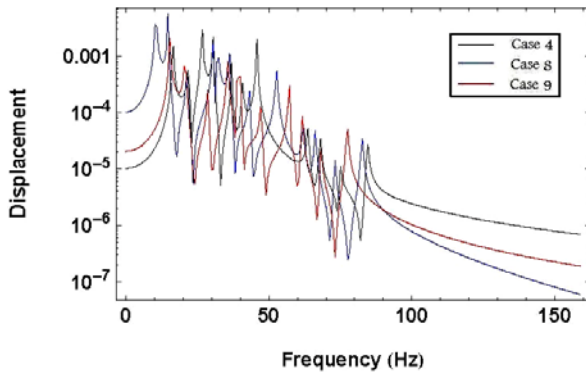


Figure 10. Frequency response of cases 4, 8 and 9

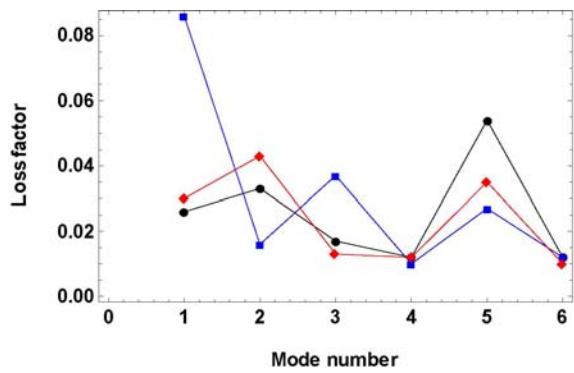


Figure 11. Modal loss factor of cases 4, 8 and 9

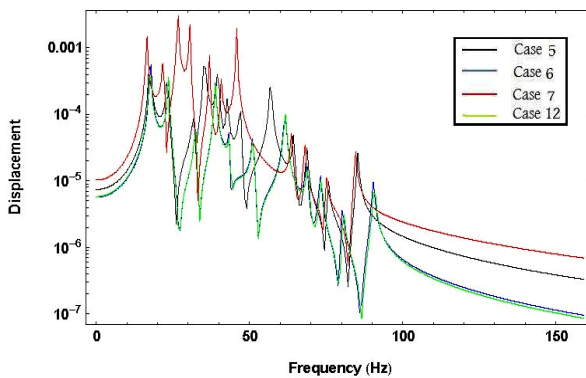


Figure 12. Frequency response of cases 5, 6, 7 and 12

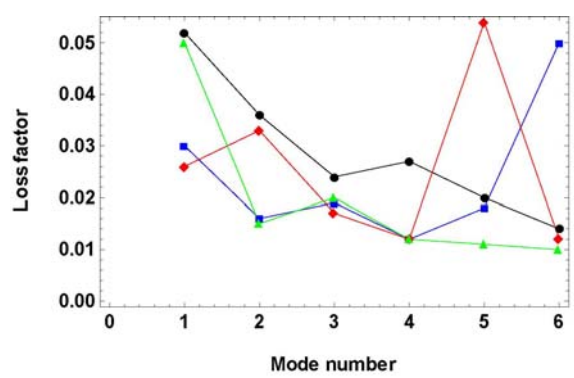


Figure 13. Modal loss factor of cases 5, 6, 7 and 12

As the last comparison we consider the frequency response function and the modal loss factors of cases 5, 6, 7 and 12. In these cases, we change the aspect ratio of the patch while the patch area remains constant. As it can be seen in Figure 12 the frequency response function of cases 6 and 12 are almost the same. The first seven natural frequencies of case 5 are higher than those of case 7, but the rest of natural frequencies are the same for these two cases. The modal loss factors of cases 6 and 12 are different specially for the first, fifth and sixth mode numbers. Also, the modal loss factor of case 7 is above other cases except for the last two mode numbers.

#### 4. Conclusion

Hamilton's principle, based on Kirchhoff thin plate theory, in conjunction with the Fourier series method are employed to study the free vibration characteristics of a simply-supported rectangular plate with an electrorheological patch. Numerical results reveal the important effects of the electric field intensity patch size and patch location on the frequency response function, natural frequencies and modal loss factors of the plate. The most important observations are as follows: using an ER patch in lower electric fields (1 Kv/mm) results in a decrease in natural frequencies. This can be due to the increase in system's total mass. But when we amplify the electric field intensity by 3 Kv/mm, the first three natural frequencies increase and using a bigger patch results in higher natural frequencies (Figures 4 and 6). The modal loss factor of the sandwich plate generally decreases when higher electric fields are applied (Figures 5 and 7). When the electric field intensity is 1 Kv/mm applying a larger patch results in a decrease in loss factors (except for the second mode), but when the electric field intensity is increased to 3 Kv/mm applying a larger patch results in an increase in loss factors (except for the fifth mode).

If we move the patch from the center of the base plate toward its corner the first two natural frequencies decrease, but when the size of the patch rises up, this change becomes less (Figures 8 and 10). When a larger patch is used moving it toward the corner of the base plate results in lower loss factors (Figure 9) but when a smaller patch is used this pattern changes (Figure 11).

To investigate the effect of the patch aspect ratio, when its area remains constant, we consider cases 5, 6, 7, 12 and Figures 12 and 13. One can see that when we change the aspect ratio of the patch, the first five natural frequencies remain unchanged, but it will have significant effects on higher natural frequencies. The modal loss factor of the plate is higher when a square patch is applied at the center of the plate.

**References**

- Choi Y., Sprecher A. F., and Conrad H., 1992 Response of electrorheological fluid-filled laminate composites to forced vibration, *J. Intell. Mater. Syst. Struct.*, **3**, 17–29.
- Coulter J. P., 1993 Engineering application of electrorheological materials, *J. Intell. Mater. Syst. Struct.*, **4**, 248–259.
- Coulter J. P., and Duclos T. G., 1989 Applications of electrorheological materials in vibration control, *Electrorheological Fluids* ed J. D. Carlson, A. F. Sprecher and H. Conrad (Lancaster, PA: Technomic) pp 300–325.
- Forsyth A. R., 1960 Calculus of Variations, Dover.
- Hasheminejad S. M., and Maleki M., 2009 Free vibration and forced harmonic response of an electrorheological fluid-filled sandwich plate, *smart Mater. And Struct.*, **18(5)**, art. no. 055013.
- Kung S. W., Singh R., 1998 Complex eigensolutions of rectangular plates with damping patches, *JSV.*, **216 (1)**, 1-28.
- Reddy J. N., 2003 *Mechanics of Laminated Composite Plates and Shells: Theory and Analysis*, New York, CRC Press.
- Saravanos D. A., and Chamis C. C., 1992 Multiobjective shape and material optimization of composite structures including damping, *AIAA J.* **30**, 805–813.
- Weiss K. D., Coulter J. P., and Carlson J. D., 1993 Material aspects of electrorheological system, *J. Intell. Mater. Syst. Struct.*, **4**, 13–34.
- Winslow W. M., 1949 Induced fibrillation of suspensions, *J. Appl. Phys.*, **20**, 1137–1140.
- Yalcintas M., and Coulter J. P., 1995 Electrorheological material based adaptive beams subjected to various boundary conditions, *J. Intell. Mater. Syst. Struct.*, **6**, 700–717.
- Yeh J. Y., Chen L. W., and Wang C. C., 2004 Dynamic stability of a sandwich beam with a constrained layer and electrorheological fluid core, *Compos. Struct.*, **64**, 47–54.
- Yeh J. Y., and Chen L. W., 2004 Vibration of a sandwich plate with a constrained layer and electrorheological fluid core, *Compos. Struct.*, **65**, 251–8.